Available online at www.sciencedirect.com
ScienceDirect
Ceramics International 38 (2012) 687–693
CERAMICS INTERNATIONAL
www.elsevier.com/locate/ceramint

Characterisation of ternary $Ti_xV_{1-x}N_y$ nitride prepared by mechanosynthesis

M.A. Roldán, M.D. Alcalá, C. Real *

Instituto de Ciencia de Materiales de Sevilla, Centro mixto US-CSIC, Av. Américo Vespucio n° 49, 41092 Sevilla, Spain

Received 11 May 2011; received in revised form 22 July 2011; accepted 25 July 2011
Available online 3rd August 2011

Abstract

In the present manuscript the authors have systematically investigated the composition and microstructure of a series of ternary nitrides ($Ti_xV_{1-x}N_y$) ($0.0 \leq x \leq 1.0$) prepared by mechanosynthesis, using XRD, SEM, EELS, XAS and TGA. The ternary titanium–vanadium nitride ($Ti_xV_{1-x}N_y$) has been obtained in all range of compositions by the mechanical treatment of the two metals under nitrogen pressure in a planetary mill with a maximum milling time of 3 h and without any post-heating treatment. The materials' microhardnesses were measured after sinterisation and compared to those reported in the literature for these types of materials. When compared with the previously reported data for bulk samples, these values are similar or higher for compositions within the range $x = 0.5$ to $x = 0.77$ ($Ti_xV_{1-x}N$).

Keywords: Mechanosynthesis; XAS; EELS; Microhardness; Ternary nitride

1. Introduction

Traditional applications of metal nitrides include cutting tools, structural materials [1,2], magnetic and electric components [3], superconducting devices [4,5] and industrial catalysts [6,7]. Ternary transition metal nitrides exhibit similar, and sometimes improved, properties to those of binary nitrides when used as electrode materials for supercapacitors and catalysts. Structural and compositional control of these materials may exert a crucial influence on their overall performance, and the formation of ternary metal nitrides may widely expand the properties of this class of materials. Despite many years of intensive effort by several research groups, the number of known ternary nitrides is trivial if compared with the known ternary oxides or sulphides. This difference is clearly due to the difficult synthesis of ternary nitrides and also to their instability with respect to that of oxides. However, after several decades of dedicated research, advances in inorganic nitride chemistry have accelerated dramatically over the past 5–10 years, and novel synthetic strategies have been developed. The traditional synthetic methods for generating these types of compounds include the amonolysis of ternary oxides [8,9] and metal alloys [10–12]; solid state reactions using chlorides, nitrates, and pre-structured oxides [13–19]; and deposition methods [20–25]. Information in the literature concerning titanium–vanadium nitride has shown the superior performance of such coated ternary compounds to those of both pure TiN and VN, with respect to their hardnesses and tribological environments [26–38]. A small addition of vanadium to titanium nitride improved the supercapacitor properties of TiN [39]. Traditionally, titanium and vanadium nitrides have been synthesised as thin films using different deposition methods, such as cathodic arc deposition [31], cathodic magnetron sputtering [32], reactive magnetron sputtering [33–35], or chemical vapour deposition, [36–38,40,41] or by the direct nitridation of metal alloys [42–45]. To our knowledge, only two works have reported the preparation of $Ti_xV_{1-x}N_y$ in bulk. Fischer et al. [46] obtained this compound by infiltrating a mixture containing the two precursor metals into mesoporous carbon nitride, heating and then decomposing the carbon nitride. In that study, mesoporous graphitic carbon nitride was used as both a nanoreactor and a reactant for the synthesis of ternary metal nitride nanoparticles. Moreover, we have previously demonstrated that this material could be obtained from the carbothermal reduction of oxide mixtures under a nitrogen atmosphere [47].

In the present study, we synthesised pure titanium–vanadium nitride by mechanically treating the two metals under nitrogen

* Corresponding author.
E-mail address: creal@icmse.csic.es (C. Real).

0272-8842/$36.00
doi:10.1016/j.ceramint.2011.07.057

pressure, in a planetary mill and with a milling time of 3 h; no post-heating treatment was applied. The final products obtained from this method were characterised and compared with the final products obtained using a thermal procedure.

2. Experimental

2.1. Materials

Vanadium (V) [262935, 99.5%, <325 mesh, Aldrich], Titanium (Ti) [93-2267, 99%, <325 mesh, Strem Chemicals] and nitrogen gas (N_2) [pure, $H_2O \leq 3$ ppm, $O_2 \leq 2$ ppm, and $C_nH_m \leq 0.5$ ppm, Air Liquide] were used as precursors.

2.2. Methods

V and Ti powders were milled under the pressure of high purity N_2 at 11 bars using a modified planetary ball mill (Fritsch, model Pulverisette 7). A steel vial of 45 cm^3 was used with 6 steel balls and 5 g of metal mixture. The diameter and the weight of the balls were 15 mm and 13.85 g, respectively, and the powder-to-ball mass ratio was 1:16. The vial was purged with N_2 several times, and the desired N_2 pressure was then adjusted prior to milling. The vial and the gas cylinder were connected through a rotary valve and a flexible polyamide tube, which allowed working pressures up to 27 bars. The rotary valve can operate up to 25 000 rpm under pressure ranging from vacuum to 70 bars. As such, the vial is permanently connected to the gas cylinder that supplies gas at its desired pressure throughout the entire process. A rotation rate of 700 rpm was always employed for the supporting disc and the superimposed vial in the opposite direction.

Characterisation of the final products (ternary nitrides) was performed using the following techniques:

1. X-ray powder diffraction (XRD). Patterns were collected with a Siemens D501 instrument equipped with a scintillation counter using Cu K_α radiation and a primary graphite monochromator. The goniometer scanning rate was of 0.4 min^{-1}. The average diameter of the coherently diffraction domain was calculated with the Scherrer method [48] using the (2 0 0) diffraction peak of $Ti_xV_{1-x}N_y$. The lattice parameter refinement corresponding to the final product was also calculated from the entire set of XRD peaks using the Lapods computer program [49] and assuming a cubic symmetry for $Ti_xV_{1-x}N_y$.
2. The iron content contamination of the milling samples was analysed by permanganimetry.
3. The composition analysis was performed with a high-resolution transmission electron microscope (HRTEM, Philips CM200, Eindhoven) with a super twin objective lens and working at 200 kV with a LaB_6 filament. The instrument is equipped with a parallel electron energy loss spectrometer (EELS, Model 766-2K, Gatan, München, Germany). For its observation, the sample was embedded in a resin, then a film of 100 nm was cut and the sample was supported on a holey carbon grid. The N, Ti and V core-loss edges were recorded in the diffraction mode with a camera length of 470 mm using a 2-mm spectrometer. The entrance aperture yielded an energy resolution at a zero-loss peak of 1.4 eV. The spectra were recorded for dark current and channel-to-channel gain variation. After subtracting the background using a standard power-law function, the spectra were deconvoluted for plural scattering applying the Fourier-ratio method and normalised to the jump. All of these treatments were performed within the EL/P program (Gatan).
4. The X-ray absorption spectra (XAS) at Ti-K ($E = 4965$ eV) and V-K ($E = 5465$ eV) edges for the sample $Ti_{0.5}V_{0.5}N_{0.94}$ were recorded at the synchrotron radiation source ESRF in Grenoble, France, at station BM29. The ring energy was 6 GeV, and the maximum stored current was 200 mA. A double crystal Si (3 1 1) monochromator was used. Higher harmonic rejection was performed by detuning both crystals by 50% of the intensity of the first harmonic. Measurements were conducted at room temperature in the transmission detection mode using detectors with 45-cm ionisation chambers that were filled with the appropriate gas mixtures. The amount of sample used was calculated to attain the optimal absorption of $\mu x = 2.5$. Because the required amount of sample was rather small (a few milligrams), it was mixed with BN to reach the minimum size to construct a self-supporting pellet.
5. Microstructural observations were conducted using scanning electron microscopy (SEM, model JSM 5400 Jeol). The images were recorded at 30 kV. The sample powders were dispersed in ethanol and supported on a metallic grid.
6. Vickers microhardness measurements (FM-700, Future-Tech, Hardness tester) were conducted on the pellet cross-sections under a load of 1 kgf for 15 s. The average microhardness was calculated from 20 indents per specimen.

3. Results and discussion

A range of ternary titanium–vanadium nitride ($Ti_xV_{1-x}N_y$) composites have been prepared by milling a mixture of these metals for different time periods under nitrogen pressure (11 bars). Fig. 1 shows the XRD pattern of the $Ti_{0.50}V_{0.50}N_{0.94}$ sample at different grinding times and the pattern corresponding to the starting metals as well. The XRD patterns indicated that titanium–vanadium nitride was formed from the mixture of the two metals by milling under nitrogen. XRD diagrams that represent 0–165 min of milling time showed Ti and V peak broadening that increased with milling time due to the refinement of the crystallite size and the formation of defects and microstrains. Moreover, the grinding between 120 and 165 min showed emergent diffraction peaks at $2\Theta = 37^\circ$ and 43° that correspond to a ternary nitride (JCPDF-89-5212). When grinding time was increased in 15 min, thus reaching 180 min, the XRD patterns evidenced only ternary nitride peaks. This result confirms that the reaction proceeded through a combustion-like process (MSR). To verify this particular, the nitrogen pressure was continuously monitored during the milling process by a SMC Solenoid Valve (model EVT307-

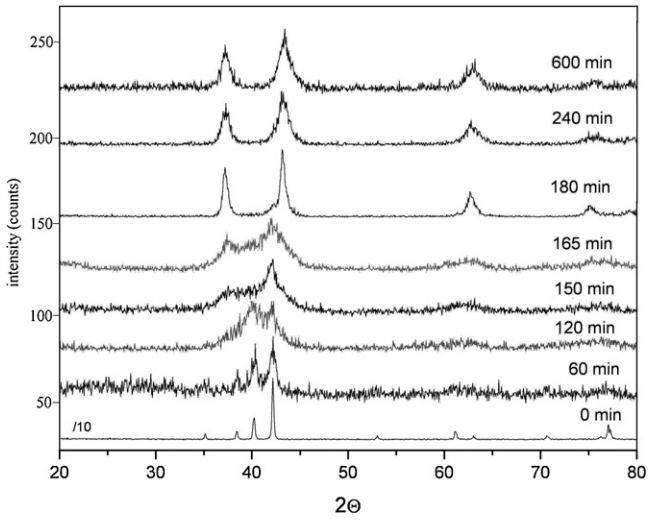

Fig. 1. XRD patterns of sample $Ti_{0.50}V_{0.50}$ at different grinding times.

5DO-01FQ, SMC Co.) that was connected to a data acquisition system ADAM-4000 series (Advantech Co. Ltd.). When the MSR occurred, the increasing temperature induced by the exothermic reaction produced an instantaneous increase in the total pressure. The ignition time of the sample (e.g., the milling time required to produce the combustion process) is deduced from the time–pressure record, being about 172 min. Additional grinding causes an increase in the nitrogen content and diffraction peaks broaden.

Fig. 2 shows the XRD pattern of sample $Ti_{0.75}V_{0.25}N_{0.96}$. When a grinding time of 4 h is applied, the nitridation reaction is initiated. The reaction continues gradually but does not get completed after 9 h of milling. This result confirms that the reaction occurs through a diffusion process.

Table 1 lists the different ternary nitride compositions, process type, ignition time and grinding time. It was possible to obtain a wide range of composites with different mechanisms.

The actual compositions were obtained by EDX using the SEM. The iron content contamination of the milling samples

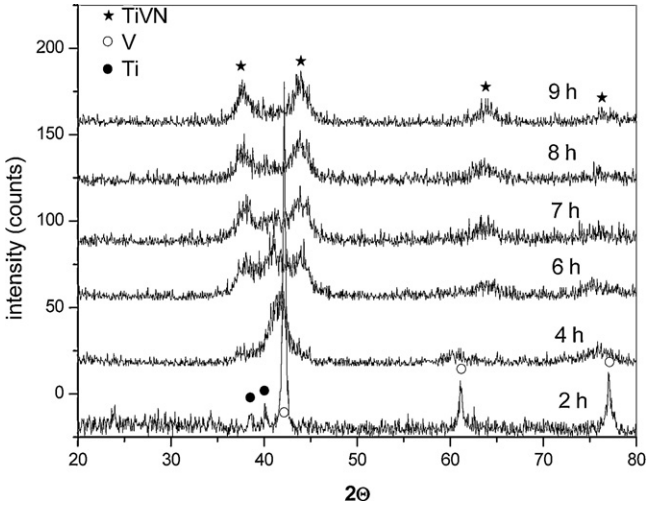

Fig. 2. XRD patterns of sample $Ti_{0.25}V_{0.75}$ at different grinding times.

Table 1
Parameters of the mechanical treatment of the Ti–V mixture under nitrogen atmosphere: grinding and ignition times and the mechanism.

Sample	Mechanism	Ignition time (min)	Grinding time (min)
$Ti_{0.86}V_{0.14}N$	Combustion	182	200
$Ti_{0.75}V_{0.25}N$	Combustion	164	200
$Ti_{0.50}V_{0.50}N$	Combustion	172	540
$Ti_{0.25}V_{0.75}N$	Diffusion	–	540
$Ti_{0.23}V_{0.77}N$	Diffusion	–	540
$Ti_{0.11}V_{0.89}N$	Diffusion	–	540

was analysed by permanganimetry, reaching a maximum value of 2.5%. The iron was completely removed by rinsing the samples with diluted hydrochloric acid. The nitriding percentage was calculated by thermogravimetric analysis (TGA), an indirect method of analysis. The TGA diagrams for the samples were recorded from room temperature to 1500 °C, at a heating rate of 5 K/min, using a nitrogen flow of 150 cm^3/min and at a pressure of 1 bar. The nitriding percentage was calculated from the mass gain, assuming a stoichiometric nitride as the final product; all results are shown in Table 2.

The considerable broadening of the ternary nitride XRD peaks in all cases suggests that this phase always exhibited a very refined microstructure. The crystallite size of the final product was estimated using the Scherrer equation, and the values are included in Table 3. The solid state reactions induced by ball milling occurred during the collisions between balls and the powder. The reaction progressed through multiple events with very short reaction times. Under these conditions, crystal growth of the new phase was hindered, generally leading to products with a nanometre microstructure. The dimension of the $Ti_xV_{1-x}N_y$ cubic unit cell was determined from the entire set of XRD peaks recorded for 2Θ values ranging from 10° to 90°. Least squares fitting of the XRD peaks was conducted with Lapods program, and the values are shown in Table 3. The lowest value obtained for the lattice parameters as compared with de Vegard́s results, suggests that a nonstoichiometric compound was obtained, and this value is in good agreement with the nitrogen percentage shown in Table 2. Studies for several transition metals with composition MN_x [50–52] have reported that the *a* parameter is very sensitive to the nitridation level.

The nitrogen content in the ternary nitride composites was also calculated using EELS analysis by recording core-level absorption edges at a microscopic level. Fig. 3 shows the N-K, Ti-L_{2-3} and V-L_{2-3} edges for the different samples prepared in

Table 2
The chemical compositions of the different ternary nitrides prepared.

Sample	Ti/V (EDX)	Composition	%Fe	%N
$Ti_{0.86}V_{0.14}N$	6.14	$Ti_{0.86}V_{0.14}N_{0.92}$	2.5	92
$Ti_{0.75}V_{0.25}N$	3.00	$Ti_{0.75}V_{0.25}N_{0.96}$	1.2	96
$Ti_{0.50}V_{0.50}N$	1.00	$Ti_{0.50}V_{0.50}N_{0.94}$	2.0	94
$Ti_{0.25}V_{0.75}N$	0.33	$Ti_{0.25}V_{0.75}N_{0.87}$	1.8	87
$Ti_{0.23}V_{0.77}N$	0.30	$Ti_{0.23}V_{0.77}N_{0.95}$	2.3	95
$Ti_{0.11}V_{0.89}N$	0.12	$Ti_{0.11}V_{0.89}N_{0.91}$	1.7	91

Table 3
The parameters obtained from the X-ray data of the prepared samples are: size particle, strain and lattice.

Sample	D (nm)	e ($\times 10^3$)	a (Å)	a (Å) Vegard
TiN	–	–	–	4.242
$Ti_{0.86}V_{0.14}N_{0.92}$	5.7	0.951	4.207	4.227
$Ti_{0.75}V_{0.25}N_{0.96}$	5.3	0.987	4.217	4.215
$Ti_{0.50}V_{0.50}N_{0.94}$	5.0	1.432	4.168	4.190
$Ti_{0.25}V_{0.75}N_{0.87}$	5.5	1.276	4.137	4.165
$Ti_{0.23}V_{0.77}N_{0.95}$	5.4	0.832	4.128	4.154
$Ti_{0.11}V_{0.89}N_{0.91}$	5.6	0.765	4.120	4.150
VN	–	–	–	4.140

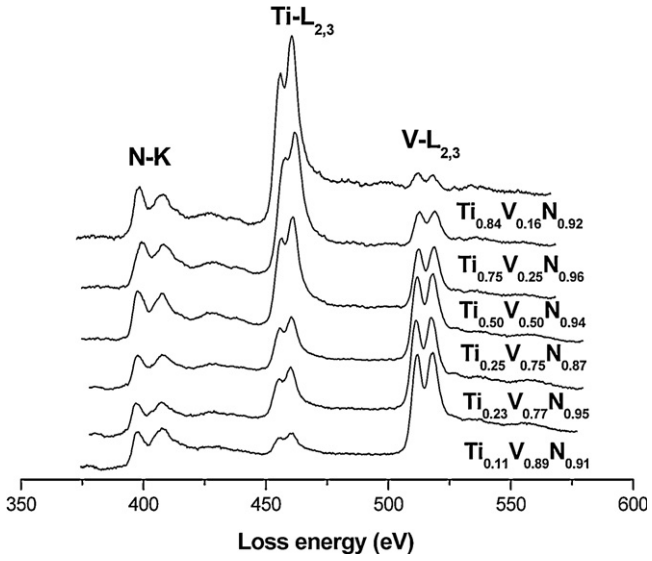

Fig. 3. N-K, Ti-$L_{2–3}$ and V-$L_{2–3}$ edges of the differently prepared ternary nitrides.

this present work. The N-K edge peak is exhibited in all samples with the same shape, indicating that the materials share the same homogeneous structure and zones with similar elemental atomic ratios. The composition of the materials was determined by integrating the number of counts under the peaks and employing the relevant cross-sections that were provided by Gatan EL/P software. The representative results from the quantitative analysis performed from Fig. 3 are shown in Table 4. The EDX and TGA values are also listed in Table 4. These results are in good agreement, and the small discrepancies between the EELS and TGA values might be explained by a percentage of the sample undergoing amorphisation; this is

Table 4
A composition comparison of the ternary nitrides obtained from different techniques.

Sample	Ti/V EDX	Ti/V EELS	Ti/N TG	Ti/N EELS
$Ti_{0.84}V_{0.16}N_{0,92}$	6.14	6.00	0.93	0.89
$Ti_{0.75}V_{0.25}N_{0,96}$	3.00	3.03	0.78	0.73
$Ti_{0.50}V_{0.50}N_{0,94}$	1.00	1.02	0.53	0.57
$Ti_{0.25}V_{0.75}N_{0,87}$	0.27	0.33	0.29	0.28
$Ti_{0.23}V_{0.77}N_{0,95}$	0.30	0.30	0.24	0.19
$Ti_{0.11}V_{0.89}N_{0,91}$	0.12	0.13	0.12	0.09

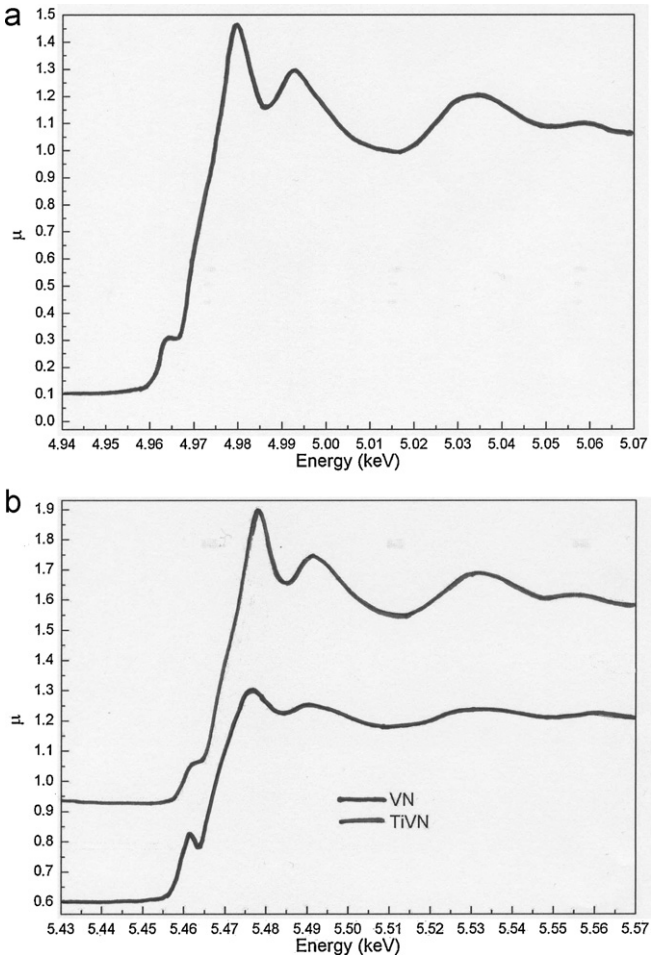

Fig. 4. Normalised XANES spectra of the following absorption edges are shown: (a) Ti-K and (b) V-K.

Table 5
The fitting EXAFS parameters of edge K-Ti for sample $Ti_{0.5}V_{0.5}N_{0.94}$. N is the coordination number (fixed to crystalline values), R is the coordination distance (calculated from the lattice parameter), σ^2 is the Debye–Waller factor (independent variable for each shell) and D is the coordination number reduction factor.

Sample	TiN-fcc (90%)				Ti metal-fcc (10%)	
D		0.56			0.99	
Lattice parameter		4.17			4.27	
Shell	1[a] (N)	2[a] (Ti)	3[a] (N)	4[a] (Ti)	1[a]	2[a]
N	6	12	8	6	12	6
R (Å)	2.09	2.95	3.61	4.17	3.02	4.27
σ (Å^2)	0.0037	0.014	0.020	0.023	0.003	0.007

Table 6
The fitting EXAFS parameters of edge K-V for sample $Ti_{0.5}V_{0.5}N_{0.94}$. The variables are described in Table 5.

Sample	VN-fcc (75%)				V metal-bcc (25%)	
D		0.73			0.99	
Lattice parameter		4.17			3.17	
Shell	1[a] (N)	2[a] (V)	3[a] (N)	4[a] (V)	1[a]	2[a]
N	6	12	8	6	8	6
R (Å)	2.09	2.95	3.61	4.17	3.02	3.17

possible because the mechanosynthesis method employed induces a high degree of amorphisation. Thus, $Ti_{0.5}V_{0.5}N_{0.94}$ was also characterised by XAS analysis; this technique can analyse both crystalline and amorphous samples. The normalised XANES spectra for the Ti-K and V-K absorption edges appeared at 4966 and 5465 eV, respectively (Fig. 4). The Ti-K and V-K edges are sensitive to the coordination environment and the oxidation states of Ti and V compounds. Therefore, the overall shape of this material was used as a fingerprint and compared with the shapes of other crystalline compounds with known structure [53]. The XANES data are similar to the spectrum obtained for TiN and VN compounds. The EXAFS

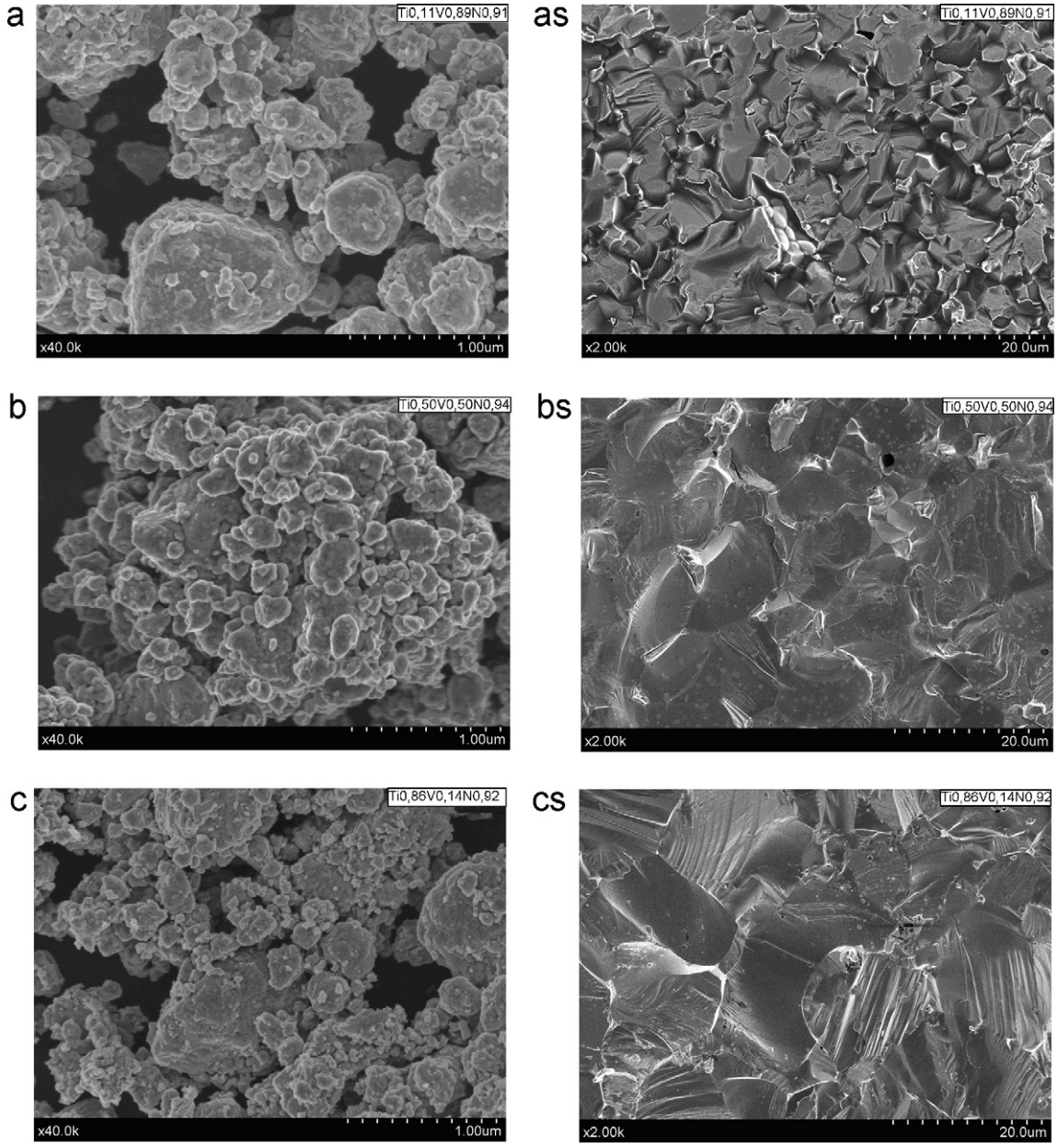

Fig. 5. SEM micrographs illustrating the morphology of three powder and sintered samples are presented with the following composition: (a) $Ti_{0.11}V_{0.89}N_{0.91}$, (b) $Ti_{0.50}V_{0.50}N_{0.94}$, and (c) $Ti_{0.86}V_{0.14}N_{0.92}$, respectively.

Table 7
The densification and microhardness of the ternary nitrides studied.

Sample	Densification (%)	Microhardness (Hv)	Microhardness (Hv) [47]
$Ti_{0.86}V_{0.14}N_{0.92}$	96	1336	1355
$Ti_{0.75}V_{0.25}N_{0.96}$	94	1425	1300
$Ti_{0.50}V_{0.50}N_{0.94}$	96	1376	1100
$Ti_{0.25}V_{0.75}N_{0.87}$	98	1166	1141
$Ti_{0.23}V_{0.77}N_{0.95}$	97	1157	1140
$Ti_{0.11}V_{0.89}N_{0.91}$	96	1277	1262

oscillation intensity of the spectra is rather low, indicating that these samples should exhibit a high degree of amorphisation. The spectra for the starting models corresponded to the crystalline structures of the species Ti-bcc, V-bcc, TiN-fcc and VN-fcc. A single free parameter a, which is the lattice parameter, was used to allow the coherent variation of the coordination distances for all coordination shells. The respective coordination numbers were fixed to those of perfect crystal structures. The Debye–Waller factors (σ^2) were allowed to vary independently for each coordination shell. Due to the highly distorted nature of these milled samples, the static disorder caused by the deformation from the ideal structure induced a coordination distance spread around the average values. This large disorder is due to the large number of defects, and a detailed explanation of the adjustment of the disorder is reported in a previous work [54]. This variable (D) ranges from 0, for a sample with atoms lacking any order even in the first coordination shell, to 1, if the sample is a perfect crystal. A summary of the results is given in Tables 5 and 6. These results are in good agreement with the results from X-ray analysis shown in Table 3.

To complete the characterisation, a morphology study of the different samples was performed using SEM. Fig. 5 displays SEM images illustrating the morphologies of three prepared samples. The microstructures of all samples were similar, being characterised by agglomerated grains with sizes ranging from 0.2 to 1 μm, formed by highly dense, spherical, nanometre sized particles.

Finally, the samples were sintered to measure their microhardness. First, green bodies were obtained as pellets that contained 400 mg of sample by isostatic pressing. The samples were then sintered at 1750 °C for 1 h under a helium atmosphere. The morphology studies for the different samples are shown in Fig. 5. A large densification, approaching full density, was observed (Table 7). The microhardness values of the current samples and those of samples previously reported using a thermal method are also shown in Table 7 [47]. These data are in good agreement with the microhardness–composition relationship, as demonstrated in the literature [28–32,35,36,55,56] for these materials. The above cited authors have shown that the compositions between $x = 0.5$ and 0.77 ($Ti_xV_{1-x}N$) correspond to the materials with the highest microhardness and that the best microhardness results correlate to sample compositions with high stoichiometry. Additionally, the microhardness values for the ternary nitride composites were lower than those obtained by these authors (2000–4000 Hv). However, all of these results correspond to films, and it is known that dense films with a high defect concentration can produce microhardness values far above those corresponding to bulk samples [55]. When these values are compared with some others previously studied for bulk samples [47], it can be seen that they are similar or higher for the compositions between $x = 0.5$ and 0.77 ($Ti_xV_{1-x}N$).

4. Conclusions

Bulk samples of ternary nitrides ranging in different compositions were rapidly obtained by mechanical treatment at room temperature. The materials richest in titanium and vanadium were produced through a combustion process in 3 h and a diffusion process in 9 h, respectively. Reactive milling is a good method to obtain these types of compounds because it is inexpensive if compared with deposition and thermal techniques. The employed characterisation methods indicate that the materials exhibited nanometre particle sizes, high sinterabilities and high microhardnesses.

References

[1] S.T. Oyama, The Chemistry of Transition Metal Carbides and Nitrides, Blackie Academic & Professional, Glasgow, Scotland, 1996, pp. 1–52.
[2] L.E. Toth, Transition Metal Carbides and Nitrides, Academic Press, New York, 1971.
[3] N. Pessall, R.E. Gold, H.A. Johansen, A study of superconductivity in interstitial compounds, J. Phys. Chem. Solids 29 (1968) 19–27.
[4] R.M. Powell, W. Skocpol, M. Tinkham, Preparation and superconducting properties of ultrafine powders and sintered compacts of nbc and nbn, J. Appl. Phys. 48 (2) (1977) 788–799.
[5] T. Yamada, M. Shimada, M. Koizumi, Fabrication and characterization of titanium nitride by high-pressure hot-pressing, Ceram. Bull. 59 (6) (1980) 611–616.
[6] S.T. Oyama, Preparation and catalytic properties of transition-metal carbides and nitrides, Catal. Today 15 (2) (1992) 179–200.
[7] H. Kwon, S. Choi, L.T. Thompson, Vanadium nitride catalysis: synthesis and evaluation for n-butane dehydrogenation, J. Catal. 184 (1999) 236–246.
[8] P.S. Herle, N.Y. Vassanthacharya, M.S. Hegde, M.S. Gopalakrishnan, Synthesis of new transition-metal nitrides, mwn(2) (m = mn, co, ni), J. Alloys Compd. 217 (1) (1995) 22–24.
[9] A. Gomathi, Ternary metal nitrides by the urea route, Mater. Res. Bull. 42 (5) (2007) 870–874.
[10] P. Krawiec, R.N. Panda, E. Kockrick, D. Geiger, S. Kaskel, High surface area V–Mo–N materials synthesized from amine intercalated foams, J. Solid State Chem. 181 (2008) 935–942.
[11] S. Korlann, B. Diaz, M.E. Bussell, Synthesis of bulk and alumina-supported bimetallic carbide and nitride catalysts, Chem. Mater. 14 (10) (2002) 4049–4058.
[12] C.J.H. Jacobsen, Novel class of ammonia synthesis catalysts, Chem. Commun. 12 (2000) 1057–1058.

[13] K.S. Weil, P.N. Kunta, J. Grins, Revisiting a rare intermetallic ternary nitride, Ni_2Mo_3N: crystal structure and property measurements, J. Solid State Chem. 146 (1) (1999) 22–35.
[14] A. El-Himri, P. Nuñez, F. Sapiña, R. Ibañez, A. Beltran, J.M. Martinez-Agudo, Synthesis of new molybdenum–tungsten, vanadium–tungsten and vanadium–molybdenum–tungsten oxynitrides from freeze-dried precursors, J. Solid. State Chem. 177 (2004) 1431–2413.
[15] Z.A. Gal, L. Cario, F.J. DiSalvo, Synthesis, structure and magnetic properties of the ternary nitride $La_3V_2N_6$, Solid State Sci. 5 (7) (2003) 1033–1036.
[16] R. Niewa, D. Zherebtsov, Z. Hu, Polymorphism of heptalithium nitridovanadate(V)$Li_7[VN_4]$, Inorg. Chem. 42 (8) (2003) 2538–2544.
[17] M.T. Barker, M.G. Francesconi, P.M. O'Meara, C.F. Baker, New synthetic routes to transition metal ternary nitrides and sulfides, J. Alloys Compd. 317–318 (2001) 186–189.
[18] S. Alconchel, F. Sapiña, D. Beltran, A. Beltran, A new approach to the synthesis of molybdenum bimetallic nitrides and oxynitrides, J. Mater. Chem. 9 (1999) 749–755.
[19] A. El-Himri, P. Nuñez, F. Sapiña, A. Beltran, Freeze-dried precursor-based synthesis of new polymetallic oxynitrides, $V_{1-u-z}Cr_uMo_z(O_xN_y)$, $V_{1-u-z}Cr_uW_z(O_xN_y)$, $Cr_{1-u-z}Mo_uW_z(O_xN_y)$ ($u,z = 0.2$, 0.33, 0.4, 0.6, $u + z < 1$), and $V_zCr_zMo_z(O_xN_y)$ ($z = 0.25$), J. Alloys Compd. 398 (2005) 289–295.
[20] H. Hasegawa, T. Suzuki, Effects of second metal contents on microstructure and micro-hardness of ternary nitride films synthesized by cathodic arc method, Surf. Coat. Technol. 188 (2004) 234–240.
[21] J.V. Ramana, S. Kumar, C. David, V.S. Raju, Structure, composition and microhardness of (Ti,Zr)N and (Ti, Al)N coating prepared by DC magnetron sputtering, Mater. Lett. 58 (2004) 2553–2558.
[22] M.B. Takeyama, T. Itoi, E. Aoyagi, A. Noya, Diffusion barrier properties of nano-crystalline TiZrN films in Cu/Si contact systems, Appl. Surf. Sci. 216 (2003) 181–186.
[23] S.M. Aouadi, J.A. Chalek, N. Namavar, N. Finnegan, S.L. Rohde, Characterization of Ti-based nanocrystalline ternary nitride films, J. Vac. Sci. Technol. B 20 (5) (2002) 1967–1973.
[24] R.L. Boxman, V.N. Zhitomirsky, I. Grimberg, L. Rapoport, S. Goldsmith, B.Z. Weiss, Structure and hardness of vacuum arc deposited multicomponent nitride coating of Ti, Zr and Nb, Surf. Coat. Technol. 125 (2000) 257–262.
[25] P. Hones, R. Sanjines, F. Levy, Electronic structure and mechanical properties of resistant coatings: the chromium molybdenum nitride system, J. Vac. Sci. Technol. A 17 (3) (1999) 1024–1030.
[26] J.H. Ouyang, S. Sasaki, The friction and wear characteristics of cathodic arc ion-plated (V,Ti)N coatings in sliding against alumina ball, Wear 257 (7–8) (2004) 708–720.
[27] J.H. Ouyang, S. Sasaki, Tribo-oxidation of cathodic arc ion-plated (V,Ti)N coatings sliding against a steel ball under both unlubricated and boundary-lubricated conditions, Surf. Coat. Technol. 187 (2–3) (2004) 343–357.
[28] N. Ichimiya, Y. Onishi, Y. Tanaka, Properties and cutting performances of (Ti,V)N coatings prepared by cathodic arc ion plating, Surf. Coat. Technol. 200 (2005) 1377–1382.
[29] K.E. Davies, B.K. Gan, D.R. McKenzie, M.M.M. Bilek, M.B. Taylor, D.G. McCulloch, B.A. Latella, Correlation between stress and hardness in pulsed cathodic arc deposited titanium/vanadium nitride alloys, J. Phys. Condens. Matter 16 (2004) 7947–7954.
[30] H. Hasegawa, A. Kimura, T. Suzuki, Microhardness and structural analysis of (Ti,Al)N, (Ti,Cr)N, (Ti,Zr)N and (Ti,V)N films, J. Vac. Sci. Technol. A 18 (3) (2000) 1038–1040.
[31] O. Knotek, W. Burgmer, C. Stoessel, Arc-evaporated Ti–V–N thin films, Surf. Coat. Technol. 54–55 (1992) 249–254.
[32] B.A. Latella, B.K. Gan, K.E. Davies, D.R. McKenzie, D.G. McCulloch, Titanium nitride/vanadium nitride alloy coatings: mechanical properties and adhesion characteristics, Surf. Coat. Technol. 200 (2006) 3605–3611.
[33] Q. Luo, Z. Zhou, W.M. Rainforth, P.Eh. Hovsepian, TEM-EELS study of low-friction superlattice TiAlN/VN coating: the wear mechanisms, Tribol. Lett. 24 (2) (2006) 171–178.
[34] U. Helmersson, S. Todoroya, S.A. Barnett, J.E. Sundgren, L.C. Market, J.E. Greene, Growth of single-crystal TiN/VN strained-layer superlattices with extremely high mechanical hardness, J. Appl. Phys. 62 (2) (1987) 481–484.
[35] O. Knotek, A. Barimani, B. Bosserhoff, F. Löffter, Structure and properties of magnetron-sputtered Ti–V–N coatings, Thin Solid Films 193–194 (1990) 557–564.
[36] R. Sanjines, C. Wiemer, P. Hones, F. Levy, Chemical bonding and electronic structure in binary VN_y and ternary $T_{1-x}V_xN_y$, J. Appl. Phys. 83 (3) (1998) 1396–1402.
[37] I.L. Singer, S. Fayeulle, P.D. Ehni, Friction and wear behaviour of TiN in air: the chemistry of transfer films and debris formation, Wear 149 (1–2) (1991) 375–394.
[38] K.N. Jallad, D. Ben-Amotz, Raman chemical imaging of tribological nitride coated (TiN, TiAlN) surfaces, Wear 252 (11–12) (2002) 956–969.
[39] D. Choi, P.N. Kunta, Nanocrystalline TiN derived by a two-step halide approach for electrochemical capacitors, J. Electrochem. Soc. 153 (12) (2006) A2298–A2303.
[40] M. Stoiber, E. Badisch, C. Lugmair, C. Mitterer, Low-friction TiN coatings deposited by PACVD, Surf. Coat. Technol. 163–164 (2003) 451–456.
[41] K.H. Habig, Chemical vapour deposition and physical vapour deposition coatings: properties, tribological behaviour and applications, J. Vac. Technol. A 4 (6) (1986) 2832–2843.
[42] S. Malinov, A. Zhecheva, W. Sha, Nitriding of titanium and aluminium alloys, Met. Sci. Heat Treat. 46 (7–8) (2004) 286–293.
[43] J.A. Garcia, G.G. Fuentes, R. Martinez, R.J. Rodriguez, G. Abrasonis, J.P. Riviere, J. Rius, Temperature-dependent tribological properties of low-energy N-implanted V5Ti alloys, Surf. Coat. Technol. 188–189 (2004) 459–465.
[44] J.A. Garcia, G.G. Fuentes, R. Martinez, A. Medrano, M. Rico, R. Rodriguez, M. Varela, I. Colera, D. Caceres, I. Vergara, C. Ballesteros, E. Roman, J.L. de segovias, Surface mechanical effects of nitrogen ion implantation on vanadium alloys, Surf. Coat. Technol. 158–159 (2002) 669–673.
[45] T. Yokoyama, K. Kobayashi, T. Ohta, A. Ugawa, An harmonic interatomic potentials of diatomic and linear triatomic molecules studied by extended X-ray-absorption fine structure, Phys. Rev. B 53 (10) (1996) 6111–6112.
[46] A. Fischer, J.O. Müller, M. Antonietti, A. Thomas, Synthesis of ternary metal nitride nanoparticles using mesoporous carbon nitride as reactive template, ACS Nano 2 (12) (2008) 2489–2496.
[47] M.A. Roldán, M.D. Alcalá, A. Ortega, C. Real, Síntesis y caracterización del nitruro ternario de titanio y vanadio ($Ti_xV_{1-x}N$), Bol. Soc. Esp. Ceram. V 50 (1) (2011) 31–40.
[48] L.E. Alexander, H.P. Klung, X-Ray Diffraction Procedures: for Polycrystalline and Amorphous Materials, John Wiley & Sons, New York, 197ϕp. 618.
[49] C. Dong, Y.J.I. Langford, LAPODS: a computer program for refinement of lattice parameters using optimal regression, J. Appl. Crystallogr. 33 (2000) 1177–1179.
[50] M.D. Aguas, A.M. Nartowski, I.P. Parkin, M. Mackenzie, A.J. Craven, Chromium nitrides (CrN, Cr_2N) from solid state metathesis reactions: effects of dilution and nitriding reagent, J. Mater. Chem. 8 (8) (1998) 1875–1880.
[51] Z.B. Zhao, Z.U. Rek, S.M. Yalisove, J.C. Bilello, Nanostructured chromium nitride films with a valley of residual stress, Thin Solid Films 472 (2005) 96–104.
[52] D. Wexler, A. Calka, A.Y. Mosbah, Ti–TiN hard metals prepared by in situ formation of TiN during reactive ball milling of Ti in ammonia, J. Alloys Compd. 309 (2000) 201–207.
[53] P. Malet, A. Muñoz-Páez, C. Martín, V. Rives, Sodium-doped V2O5/TiO2 systems: an XRD, DTA, TG/DTG, IR, V-UV, TPR, and XANES study, J. Catal. 134 (1992) 47–57.
[54] V. López-Flores, M.A. Roldán, C. Real, A. Muñoz Páez, G.R. Castro, Polymorphic transformation from body-centered to face-centered cubic vanadium metal during mechanosynthesis of nanostructured vanadium nitride determined by extended x-ray absorption fine structure spectroscopy, J. Appl. Phys. 104 (2008) 023519.
[55] J.E. Sundgren, H.T.G. Hentzell, A review of the present state of art in hard coatings grown from the vapour phase, J. Vac. Sci. Technol. A 4 (5) (1986) 2259–2262, 279.
[56] H.C. Barshilia, K.S. Rajam, Nanoindentation and atomic force microscopy measurements on reactively sputtered TiN coatings, Bull. Mater. Sci. 27 (1) (2004) 35–41.